

# One Novel Control Strategy for AC-DC-AC Converter Without DC Link Electrolytic Capacitor

Shihong Xie

School of Electrical and Information Engineering  
Shaanxi University of Science & Technology  
Xi'an, China  
e-mail: xierthy@126.com

Yanjing Meng

School of Electrical and Information Engineering  
Shaanxi University of Science & Technology  
Xi'an, China  
e-mail: yjm1292@163.com

**Abstract**—A novel control strategy for ac-dc-ac converter without electrolytic capacitor is proposed to settle the disadvantage of the traditional converter caused by large electrolytic capacitors. This study is developed in four parts: first, after analyzing for the large electrolytic capacitor defect, one novel electrolytic capacitor-less converter and its control strategy are proposed; second, the efficiency of voltage conversion for the novel converter is deduced and compared with the conventional converter, third, the mathematics model of the converter is built; forth, some simulation tests are carried out to verify the performance of converter. The simulation results show that the proposed converter is valid.

**Keywords**—Converter; Electrolytic Capacitor; Six-Pulse Voltage; Mathematic Model; Energy Feedback

## I. INTRODUCTION

THE traditional voltage ac-dc-ac converters have been widely used in many domains. In view of filtering and energy saving, many large electrolytic capacitors are often connected to the DC link of the traditional converter. But these electrolytic capacitors have many disadvantages such as big volume, high cost and short life<sup>[1-4]</sup>. These disadvantages will result in the converter losing efficacy. So, one novel converter without electrolytic capacitor is considered as a solution for the disadvantages of the traditional converter.

Numerous articles explore the solution in recent years. One topology of electrolytic capacitor-less converter was presented in [5-6]. One feed-forward compensation control scheme is applicable to resist the influence of improper input voltages in [5]. The resistance-inductance load but three-phase induction motor load tested in the article couldn't completely verify the performances of the supposed converter. One proportional-Resonant control of a single-phase to three-phase converter without electrolytic capacitor is proposed in [6]. But power of the converter with a single-phase input power source is limited in [5-6]. In [7], one energy feedback system built on amplitude and phase control Sinusoidal Pulse wide modulation (SPWM) technology was putted forward. The system could improve the control performance of energy feedback current, but employed the double quantity of electrolytic capacitors of the traditional converter. In [8], a direct ac-ac converter connected by high frequency transformer is proposed. This converter could

serve as one phase or three phases energy conversion equipment. Nonetheless, the volume of the high frequency transformer restricted the largest power of this converter. On the other hand, electrolytic capacitor also exists in this converter. Contrasting to above schemes, one ac-dc-ac converter without dc link electrolytic capacitor proposed in [9-10] gets a better scheme to settle these disadvantages of the traditional converter. This converter includes two back-to-back voltage source inverters and there is only a five microfarad ceramic capacitor in its dc link. Nonetheless, the dynamic deviation of the dc link voltage reaches twenty volts that isn't a favorable performance. In [11-12], other circuit topologies of converter without electrolytic capacitor are also proposed, but main content is to study power-decoupling of a multi-port isolated converter in [11], and the theme is to solve the high-frequency pulsating of three-phase converter in [12].

Inspired by above articles, the paper presents an electrolytic capacitor-less converter that its dc link voltage is six pulse voltage. The first content is to analyze the fundamental function of the dc link electrolytic capacitor and put the novel converter topological structure. The second content is to deduce the voltage conversion efficiency of the proposed converter. And the third is to build the model of the converter-motor system and test the performance of the system.

## II. THE CONVERTER WITHOUT ELECTROLYTIC CAPACITOR

### A. the analysis for dc link electrolytic capacitor of the traditional converter

DC link electrolytic capacitors of the conventional voltage source ac-dc-ac converter have two fundamental functions. The first is voltage smoothing. The output voltage of the front-end rectifier of the converter is a pulsation dc voltage. The voltage rectified by six diodes consists of six sinusoid-heads in one power source period and contains the heavy harmonic. However, one constant dc voltage is expected to the inverter of the conventional converter. Many electrolytic capacitors can be paralleled on the dc link of the converter to smooth the pulsation dc voltage. The second function of electrolytic capacitor for the traditional converter is energy stockpiling. When instantaneous value of the input ac line voltage of the traditional converter feeding a

induction motor is larger than the value of dc link voltage, the front-end rectifier is in on work, the input power source feeds the electrolytic capacitors and load. On the contrary, the front-end rectifier is disabled and the electrolytic capacitors feeds the motor. On another condition, when the motor is reducing speeds, the stator voltages are higher than the dc link voltage and energy feeds back to the electrolytic capacitors. So, above two functions should be disposed in another new converter system in that the electrolytic capacitors are removed from the dc link of converter.

**B. The converter topology**

One novel electrolytic capacitor-less converter topology is showed in figure 1. Power-side rectifier is composed of six diodes. And the load-side inverter is composed of six insulated gate bipolar transistors(IGBT) and every IGBT is severally paralleled with a backward diode. The differences of the novel converter comparing with the traditional is that capacitor C paralleled on the dc link is a small non-polarity thin-film capacitor and every IGBT of the power-side inverter is paralleled with a resistance-capacitor protection circuit. The small capacitor is expected to absorb the peak voltage generated by switching action. Basing the purpose of the novel converter, energy from the motor can be fed back to the power grid and a dc link six-pulse voltage composing of six sinusoid-heads in one period can be maintained.

The power-side inverter feeding energy back to the power grid can be controlled with a simple method. The power-side inverter will be triggered only when the dc link voltage pumped by the feedback energy is greater than the expected six-pulse value. The control principle is that the IGBT corresponding with the conductive diodes of the power-side rectifier will be triggered. For example, when the diodes of A-phase up bridge arm and B-phase down bridge arm of the power-side rectifier are conductive, the dc link voltage is equal to input line voltage  $U_{AB}$ . If motor energy starts to feed back to capacitor C, dc link voltage will be higher than the input line voltage  $U_{AB}$ , the above conductive two diodes will be turn-off naturally and the IGBT of A-phase up bride arm and B-phase down bridge arm of the power-side inverter will be triggered.

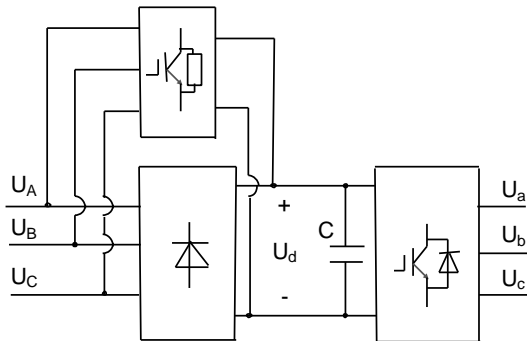


Figure 1. Topology of converter without electrolytic capacitor

**C. Voltage conversation efficiency of the novel inverter**

In order to analyze the output voltage of the novel converter, voltage conversation efficiency is defined as the following.

$$\eta = \frac{U_o}{U_i} \tag{1}$$

In this equation,  $U_o$  is the effective value of fundamental wave of the output voltage and  $U_i$  is the phase voltage effective value of the three phases input voltages of the converter.

The space vector pulse width modulation(SVPWM) technology can be used to enhance the voltage conversation efficiency and reduce the output voltage harmonic. Basing this technology, the triggering time of every IGBT device will be computed precisely in accordance with the instantaneous dc link voltage. Hence, the disturbance caused by the change of dc link voltage has been restrained. On the other hand, the harmonic generated by the sampling period is further reduced because the switch frequency of IGBT is higher than the frequency of input voltage. Many presented papers verify the performance of the SVPWM method[13-14].

Space voltage vector is defined as the following.

$$v_s = \sqrt{\frac{2}{3}}(u_a + u_b e^{jr} + u_c e^{j2r}) \tag{2}$$

In this equation,  $r$  is equal to two thirds  $\pi$ .

If  $u_a$ ,  $u_b$ , and  $u_c$  are three-phase balanced voltages, the following equation can be acquired.

$$\begin{aligned} v_s &= \sqrt{\frac{2}{3}} \left[ U_m \cos(\omega t) + U_m \cos(\omega t - \frac{2\pi}{3}) e^{jr} + U_m \cos(\omega t + \frac{2\pi}{3}) e^{j2r} \right] \\ &= \sqrt{\frac{3}{2}} U_m e^{j\omega t} \\ &= V_s e^{j\omega t} \end{aligned} \tag{3}$$

In this equation,  $U_m$  is the amplitude of the phase-voltage,  $V_s$  is the amplitude of the space voltage vector.

The switching vector of the inverter up-arms is defined as  $(S_a, S_b, S_c)$ . When A-phase up-arm IGBT is triggered and A-phase down-arm IGBT will be closed,  $S_a$  is equal to one. On the contrary,  $S_a$  is equal to zero. The means of  $S_b$ , and  $S_c$  are consistent with  $S_a$ . The output voltage vector of the converter can be signed  $v_i$  ( $i=0,1,2...6,7$ ).  $v_0$  and  $v_7$  are two zero vectors. Another six vectors are nonzero vectors drawn in figure 2. The nonzero vectors are defined as the following.

$$v_i = \sqrt{\frac{2}{3}} u_d e^{j(i-1)\frac{\pi}{3}}, \quad (i=1,2\dots6) \quad (4)$$

$$\frac{\sqrt{3}}{2} \leq \eta \leq 1 \quad (7)$$

In this equation,  $u_d$  is the dc link voltage of the converter.

The size of  $u_d$  is set as the amplitude and  $\omega_1 t$  is set as the argument of a variable in another two-phase static coordinate system named  $\alpha_2$ - $\beta_2$  coordinate system. The track of  $u_d$  is the envelope line shown in figure 2. In this coordinate system, zero time reference is set in the time that the amplitude of  $u_d$  reaches the largest value. The angle between  $\alpha_1$  and  $\alpha_2$  is signed as  $\theta$ , which indirectly reflexes the phase-difference of output voltage and input power source of the converter. The effective range of  $\theta$  is between zero and one third  $\pi$ .

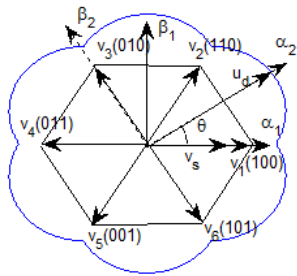


Figure 2. Dc-link voltage and space voltage vector

If the track of magneto-motive force generated by  $v_s$  is rounded, the track of  $v_s$  must also be rounded. The largest track of  $v_s$  is the in-circle of the hexagon forming with six nonzero vectors shown in figure 2. So, the following formula can be reasoned.

$$V_{smax} = \frac{\sqrt{3}}{2} |v_i| = \frac{1}{\sqrt{2}} u_d \quad (5)$$

In this equation,  $V_{smax}$  is the largest amplitude of  $v_s$ .

But dc link voltage of the novel converter is a six-pulse voltage, and the voltage changes between  $3U_m/2$  and  $\sqrt{3}U_m$ . So, the largest amplitude range of  $v_s$  is shown as the following formula.

$$\frac{3}{2\sqrt{2}} U_m \leq V'_{smax} \leq \frac{\sqrt{3}}{\sqrt{2}} U_m \quad (6)$$

In this equation, the cause of the maximum amplitude changing is the phase difference between input voltage and output voltage. That is to say the cause is  $\theta$ . If  $\theta$  is equal to  $\pi/6$ ,  $V'_{smax}$  will reach the maximum value. Similarly, if  $\theta$  is equal to zero,  $V'_{smax}$  will reach the minimum value. So, the voltage conversation efficiency of the novel converter can be calculated by using (3) and (6).

In conclusion, the voltage conversation efficiency of the novel converter is influenced by the phase difference of input voltage and output voltage, but the maximum efficiency is equal to the efficiency of the traditional converter.

#### D. Converter mathematics model

When dc link voltage of the novel converter is six-pulse voltage, it will be calculated in the following equation.

$$u_d = k_A u_A + k_B u_B + k_C u_C \quad (8)$$

In this equation,  $k_A$ ,  $k_B$  and  $k_C$  are the conversion function of the power-side rectifier shown in figure 1. They can be calculated by the following equation.

$$k_j = \begin{cases} 1, u_j = \max(u_A, u_B, u_C) \\ 0, \min(u_A, u_B, u_C) < u_j < \max(u_A, u_B, u_C) \\ -1, u_j = \min(u_A, u_B, u_C) \end{cases} \quad (9)$$

In this equation,  $j$  is equal to  $A, B, \text{ or } C$ .

For the novel converter, when  $k_A$  is equal to one,  $k_B$  is equal to negative one,  $k_C$  is equal to zero and  $v_i$  is equal to  $v_1$  or  $v_6$ , the equivalent circuit model of converter-motor system is shown in figure 3. The equivalent circuit in other switch states can also be acquired by the same methods.

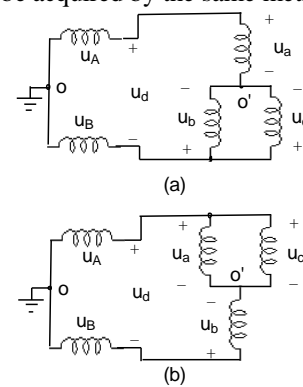


Figure 3. Inverter equivalent circuit

Supposing that an induction motor is fed by the novel converter. Every phase voltage can be derived from the figure 3. In figure 3(a), three phase-voltages can be computed by using the following equation.

$$\begin{cases} u_a = \frac{2}{3} u_d \\ u_b = u_c = -\frac{1}{3} u_d \end{cases} \quad (10)$$

In figure 3(b), these voltages can be acquired in the following equation.

$$\begin{cases} u_a = u_c = \frac{1}{3}u_d \\ u_b = -\frac{2}{3}u_d \end{cases} \quad (11)$$

With the same method, three phase-voltages can be unified in one equation as the following.

$$\begin{bmatrix} u_a \\ u_b \\ u_c \end{bmatrix} = \frac{u_d}{3} \begin{bmatrix} 2 & -1 & -1 \\ -1 & 2 & -1 \\ -1 & -1 & 2 \end{bmatrix} \begin{bmatrix} S_a \\ S_b \\ S_c \end{bmatrix} \quad (12)$$

Math model of the novel converter can be acquired by using (9) and (12) as the following formula.

$$\begin{bmatrix} u_a \\ u_b \\ u_c \end{bmatrix} = \frac{1}{3} \begin{bmatrix} k_A(2S_a - S_b - S_c) & k_B(2S_a - S_b - S_c) \\ k_A(2S_b - S_a - S_c) & k_B(2S_b - S_a - S_c) \\ k_A(2S_c - S_a - S_b) & k_B(2S_b - S_a - S_c) \end{bmatrix} \begin{bmatrix} u_A \\ u_B \\ u_C \end{bmatrix} \quad (13)$$

In this equation,  $(u_A, u_B, u_C)$  is the input voltage of the converter,  $(u_a, u_b, u_c)$  is the output voltage of the converter,  $(k_A, k_B, k_C)$  is the conversation function of the power-side rectifier and  $(S_a, S_b, S_c)$  is the switch function of the load-side inverter.

### III. SIMULATION AND ANALYSIS

#### A. Simulation of converter driving resistance-induction load

Simulation system is built to verify the performance of the novel converter. The converter drives a resistance-induction load, which is consisted of a resistance and a induction. The resistance is zero point five ohm and the induction is 10 millihenry. The SVPWM technology is used to control the load-side inverter of the converter and the switch frequency of the inverter is ten thousands hertz. Input voltage of the converter is three hundred and eighty voltage. Frequency of input voltage is fifty hertz. Output voltage size is linearly acted in line with it's the frequency. The parameter of film-capacitor is thirty three microfarad. The parameter of electrolytic capacitor of the traditional converter is four thousands and seven hundreds microfarad, which is developed by the target that wave voltage are less than five percent. Simulation software is Matlab R2014a. Simulation algorithm is ode23tb and maximum step is ten microsecond.  $\theta$  showed in figure 2 is one-sixth  $\pi$ .

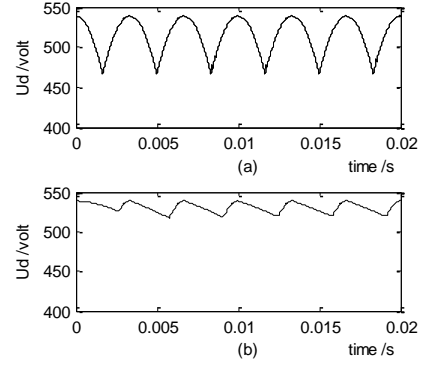


Figure 4. Contrast of dc-link voltage of two converters with resistance-inductance load

The simulation results are shown in figure 4 and table 1. Figure 4(a) is the dc link voltage of the novel converter. Corresponding to figure 4(a), figure 4(b) is the voltage of the traditional converter. When the frequency of output voltage changes from five hertz to fifteen hertz, thirty hertz and fifty hertz, the effective values of the output voltage fundament component, the harmonic sizes and the maximum conversation efficiency are shown in table 1.

TABLE I. PERFORMANCE CONTRAST OF TWO CONVERTER WITH SAME LOAD OF RESISTANCE AND INDUCTANCE

Item	Frequency	New converter	Traditional converter
THD	5 Hz	31.1	30.8
	15Hz	11.1	11.2
	25 Hz	8.1	6.9
	50 Hz	0.8	4.0
$U_{ab}(V)$	5 Hz	40.1	42
	15Hz	115	119.2
	25 Hz	189.8	196.8
	50 Hz	380.9	366.5
$\eta$	50 Hz	1.0	0.96

#### B. Simulation of converter driving induction motor

In order to further test the performance of the novel converter, an induction motor is driven by the novel converter and the traditional converter. Vector control technology is employed in this converter-motor system. A break resistance is paralleled on dc link of the traditional converter. The parameters of two converters and simulation condition are identical as the previous.

Simulation results are shown in figure5-7 and table 2. Figure 5 shows the speed response of a motor fed by above two converters. Figure 6 shows the dc link voltage of above two converters. Figure 7 shows the electromagnetic torque responses. When the frequency of the output voltage changes from five hertz to fifteen Hertz, twenty five hertz and fifty hertz, the effective values of the output voltage fundament component, the harmonic sizes and the maximum conversation efficiency are shown in table 2.

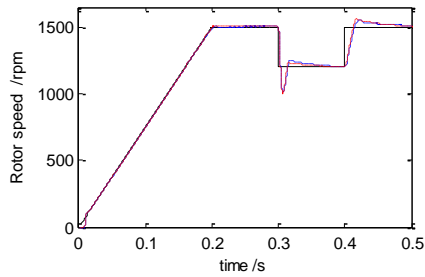


Figure 5. Contrast of speeds of a motor fed by two converters with vector control

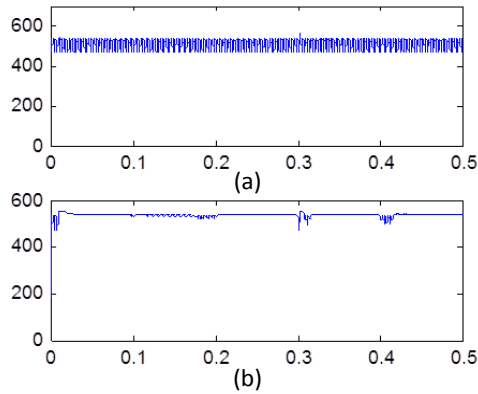


Figure 6. The dc link voltages of two converters with a motor load. (a) the novel. (b) the traditional

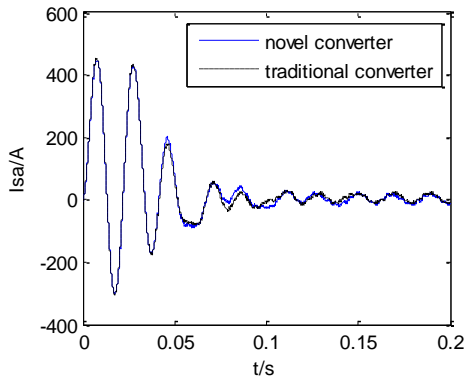


Figure 7. Stator current response of induction motor starting process

TABLE II. PERFORMANCE CONTRAST OF TWO CONVERTERS WITH A MOTOR LOAD

Item	frequency	New converter	Traditional converter
THD (%)	5 Hz	19.4	14.6
	15Hz	11.2	6.97
	25 Hz	6.73	6.2
	50 Hz	37.7	3.5
U <sub>ab</sub> (V)	5 Hz	41.5	40.3
	15Hz	118.1	117.1
	25 Hz	194.1	189.4
η	50 Hz	386.8	385.4
	50 Hz	1.02	1.01

C. Simulation tests about mathematic model

Some tests based on the mathematics model are intended to verify the veracity of the mathematical model of the novel converter. On the contrast, another tests based on the novel converter are further implemented, which is built by SimPowersystem toolbox. Testing condition is same. Simulation results are shown in figure 8 and table 3. Figure 8(a) is the output line-voltage of the converter basing on the topology. On the contrast, figure 8(b) is the output line voltage of the converter based on mathematics model. Fundamental wave effective value along with harmonic of output line voltage is shown as table 3.

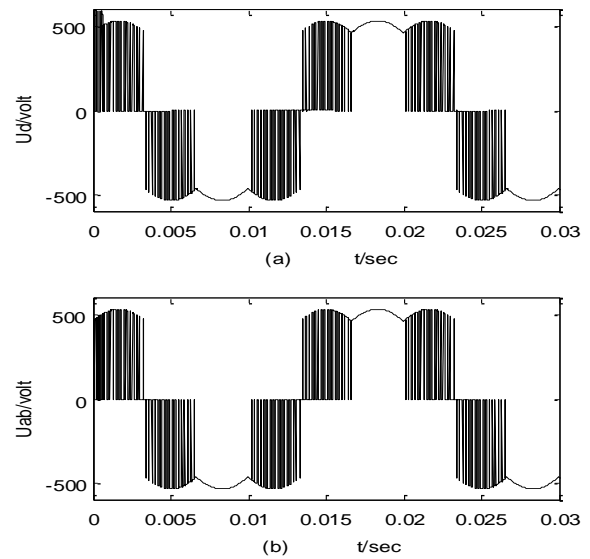


Figure 8. Output voltage of two models of converter. (a) The mathematical model. (b) the novel converter

TABLE III. HARMONIC OF OUTPUT VOLTAGE OF CONVERTER

Item	frequency	Basing on the mathematic model	Basing the topology
THD(%)	10 Hz	2.8	1.79
	25 Hz	0.94	0.49
	50 Hz	0.2	0.22
U <sub>o</sub>	10 Hz	76.37	76.09
	25 Hz	190.1	190.5
	50 Hz	379.6	379.8

D. The results analyzing

Figure 4 shows that the voltages on dc link fit the expected voltages for two converters. Figure 4(a) demonstrates that the dc link voltage of the novel converter is six-pulse wave voltage. Figure 4(b) demonstrates that the dc link voltage of the traditional converter is an approximately constant dc voltage, whose ripple is less than five percent.

Figure 5 shows that the rotor speed performance of an induction motor fed by the novel converter is same as the traditional.

Figure 6 shows that the dynamic error of the dc link voltage of the novel converter driving an induction motor is smaller than the traditional. Figure 6(a) demonstrates that the dc link voltage of the novel converter maintains six-pulse voltage. However, figure 6(b) demonstrates that the dc link voltage of the traditional converter has a larger error than the novel converter.

Figure 7 shows that A-phase stator currents of an induction motor fed by two different converters have the same performance.

Data in table 1 show that the maximum voltage conversion efficiency of the novel converter is equal to the traditional. The harmonic and the output voltage at different frequency of the novel is similar to the traditional.

Data from table 2 except the harmonic of the output voltage at fifty frequency show that the novel converter has the similar performance with the traditional.

Output voltage in figure 8 and the data in table 3 show that the mathematical model of the novel converter has the same performance with the novel converter. So the model is accurate.

#### IV. CONCLUSION

The electrolytic capacitor-less ac-dc-ac converter proposed in this paper has the following characteristic.

(1) The novel topology is effective for driving an induction motor.

(2) The dc link voltage is a six-pulse voltage.

(3) the harmonic of the output voltage caused by the six-pulse voltage on dc link is similar to the traditional.

(4) the voltage conversion efficiencies of the novel converter feeding two different loads are equal to the traditional.

(5) Simulation results show that the mathematics model of the novel converter is accurate and easy to build.

#### ACKNOWLEDGMENT

This work was supported by China Nature Science Foundation(51577110)

#### REFERENCES

- [1] Lu Xiwei Liu Zhigang Wang Lei. Estimate Approach for Fatigue Damage of Aluminum Electrolytic Capacitor Based on Accumulated

Damage Theory[J]. Transactions of China Electro technical Society, 2011,(04):13-18. Doi:10.19595/j.cnki.1000-6753.tces.2011.04.003

- [2] Niu, H., Wang, S., Ye, X., et al. "Lifetime prediction of aluminum electrolytic capacitors in LED drivers considering parameter shifts," Oct.Vol.(88-90),2018, 453-457, DOI: 10.1016/j.microrel.2018.06.027
- [3] Hadeed Ahmed Sher, Khaled E. Addoweesh, Yasin Khan. Effect of short circuited dc link capacitor of an ac-dc-ac inverter on the performance of induction motor[J].Journal of King Saud University – Engineering Sciences,2016,28: 199–206.
- [4] Hadeed A Shera, Khaled E Addoweesh, Zorays Khalid, etc. Theoretical and experimental analysis of inverter fed induction motor system under DC link capacitor failure[J]. Journal of King Saud University- Engineering Sciences,2015,06 (001) :1-9.
- [5] DAI Bin, ZHAO Run-lin, SHANG Dong-juan. Research on Output Control of High-performance Single-phase Voltage-source Inverters[J]. Electrical Measurement & Instrumentation, 2011,48(01):42-45.doi: 1001-1390(2011)01 -0042 -04.
- [6] H. Luo, G.P. Wu, Q Yin, "Proportional-resonant control of a single-phase to three-phase converter without electrolytic capacitor," Proc. 2015 Chinese Automation Congress(CAC 2015), Nov. 2015, pp. 1798-1803,DOI: 10.1109/CAC.2015.7382795
- [7] Zhang Chenghui, Li Ke, Du Chunshui,etc. An Energy-Feedback Control System of Inverter Based on Phase and Amplitude Control[J]. Transactions of China Electrotechnical Society,2005,20(2):41-45. DOI : 10.19595/j.cnki.1000-6753.tces.2005.02.007
- [8] Hemalatha S, A. Maheswari. DIRECT AC-AC CONVERTER WITH HIGH FREQUENCY LINK TRANSFORMER USING SINUSOIDAL PWM TECHNIQUE[J]. South Asian Journal of Engineering and Technology Vol.2, No.20 (2016) 51–56.
- [9] Kim Joohn Sheok, Sul Seung Ki. New control scheme for AC-DC-AC converter without DC link electrolytic capacitor[J].IEEE Annual Power Electronics Specialists Conference, p 300-306, 1993
- [10] C.C. Hou, H.P. Su, "multi-carrier PWM for AC-DC-AC converter without DC link electrolytic capacitor," 2014 International Power Electronics Conference(IPEC-Hiroshima-ECCE Asia 2014), May 2014, pp. 2821-2825, DOI: 10.1109/IPEC.2014.6870081
- [11] M.S. Irfan, J.H. Park, "Power-Decoupling of a Multiport Isolated Converter for an Electrolytic-Capacitorless Multilevel Inverter," IEEE TRANSACTIONS ON POWER ELECTRONICS, 2018, 33, (8), pp. 6656-6671. DOI: 10.1109/TPEL.2017.2763168
- [12] Montie A. Vitorino, Luciano F. S. Alves, F.M.P. Italo Roger, et al, "High-frequency pulsating DC-link three-phase inverter without electrolytic capacitor," Conf. Proc. IEEE Appl. Power Electron. Conf. Expo.(APEC 2017), March 2017, pp. 3456-3461, DOI: 10.1109/APEC.2017.7931193
- [13] LU Yuan, HU Binghui, ZHANG Junwei, etc. A three-segment algorithm research based on SVPWM modulation[J]. Power System Protection and Control, 2016, (06) :68-75.
- [14] Zhou Juan Wei Chen Yang Yu,etc. Inverter Simplified Algorithm of PWM and Inhibit Common-Mode Voltage Strategy[J]. Transactions of China Electro technical Society, 2014,(08):158-165.